BIOCHEMICAL AND BIOPHYSICAL RESEARCH COMMUNICATIONS **237,** 16–23 (1997)
ARTICLE NO. RC977062

Characteristics of Glutathione-Capped ZnS Nanocrystallites

Weon Bae,* Rizwana Abdullah,* David Henderson,† and Rajesh K. Mehra*,†,[1]
Environmental Toxicology Graduate Program and †Department of Entomology, University of California, Riverside, California 92521

Received June 18, 1997

The titration of increasing equivalents of inorganic sulfide into preformed Zn-glutathione led to the appearance of UV/VIS spectral features attributable to ZnS nanocrystallites. Glutathione-ZnS complexes upon irradiation caused reduction of methylviologen confirming their semiconductor properties. Size-fractionation of glutathione-ZnS samples on a gel filtration column showed the formation of a range of complexes whose spectral properties were correlated with the sulfide content. The stoichiometry of Zn:glutathione increased from 1:2 to a maximum of about 7:1 as the sulfide/Zn ratios increase from 0 to ~1.0 in Zn-glutathione complex indicating up to 14-fold increase in the Zn-binding capacity of glutathione upon sulfide incorporation. Spectral characteristics of GSH-capped ZnS nanocrystallites were significantly influenced by pH and by the stoichiometry of Zn, sulfide and glutathione in the complex. Samples containing least glutathione and highest sulfide showed maximal luminescence at pH 6, whereas those with higher glutathione and lower sulfide content showed maximal luminescence at pH 11. © 1997 Academic Press

The tripeptide glutathione (GSH) occurs at mM concentrations in most living cells and participates in a variety of physiological reactions such as (i) conjugation of xenobiotics for eventual elimination (1), (ii) maintenance of redox status (2) and (iii) sequestration of potentially toxic metal ions (3). GSH temporarily complexes metal ions prior to the synthesis of metal-sequestering peptides/proteins like phytochelatins (PCs) and metallothioneins (4-7). The metal ions are subsequently donated by GSH to PCs or metallothioneins. $Cd_1(GSH)_2$ complex was recently shown to be critical for the expression of Cd tolerance and transport of this toxic metal ion to vacuoles in *Saccharomyces cerevisiae* (8). Another role for GSH in metal detoxification reactions involves the conversion of this tripeptide into PCs which have a higher metal-binding affinity and capacity than GSH (4-6). The Cd-binding capacity of PCs (9) and of GSH (10) is substantially increased upon incorporation of inorganic sulfide into Cd-GSH or Cd-PC complexes. These complexes are crucial for metal detoxification as the *Schizosaccharomyces pombe* mutants lacking the ability to make the so-called high molecular weight PC-CdS complexes exhibit Cd sensitivity (11-13). PC-CdS and GSH-CdS complexes also possess unique optical properties similar to those of CdS semiconductor nanocrystallites (9,10,14). Recent studies suggest that CdS semiconductors may be used for free-radical mediated degradation of organic contaminants in waste-waters (15,16). However, Cd is highly toxic and its use in waste-water treatment is unlikely to be an acceptable remediation technology.

Zn complexes of GSH have been studied extensively (17), although it is unknown whether Zn-GSH complexes can incorporate sulfide and if such complexes will exhibit nanocrystalline nature. It has been shown that GSH-CdS complexes are formed prior to the synthesis of PC-CdS species (18). Thus, studies on GSH-metal-sulfide complexes are important to understand the fundamental mechanism involved in metal sequestration. We show here for the first time that Zn-GSH forms a variety of GSH-ZnS complexes with nanocrystalline properties. These properties can be easily altered by changing the sulfide/Zn ratios and consequently the GSH content of these nanocrystallites.

MATERIALS AND METHODS

Reagents. Reduced GSH (99%) was purchased from Alexis. Glutathione-reductase, NADPH, Sephadex G-10, Sephadex G-25 and 2,2′dithiodipyridine were from Sigma. Methylviologen was procured from Acros. All other routine chemicals were obtained from Fisher Scientific.

Titration of sulfide into GSH. The incorporation of inorganic sulfide into Zn-GSH was initially determined by sulfide-induced changes in the absorption spectrum. $ZnSO_4$ (in 0.01 N HCl) was mixed with GSH (in 0.1% TFA) to achieve Zn/GSH molar ratios of

[1] Corresponding author. Fax: 909-787-3087. Email: Rajesh.Mehra@UCR.EDU.

0006-291X/97 $25.00

0.5 and 1.0. The samples were transferred to an anaerobic chamber (Plaslabs) and the pH was adjusted to 8.6 using Tris.Cl (0.25 M, final concentration). The reconstituted Zn-GSH was brought out of the chamber and titrated with 0-2.0 mol eq. of sulfide using a standardized solution of sodium sulfide. It was critical to mix samples rapidly while sulfide was added. Slow addition of sulfide led to the formation of localized precipitates. Excess sulfide was removed by thorough degassing and saturation with N_2. The samples were then scanned on a double beam UV/VIS spectrophotometer (Perkin-Elmer Lambda 3) controlled by PECSS software.

Gel-filtration fractionation of GSH–ZnS complexes. Zn-reconstituted GSH (Zn:GSH::1:2) samples were titrated with 0, 0.5, 1.0 and 2.0 equivalents of inorganic sulfide as mentioned above. The final Zn concentration in these samples was 25 mM and 2.0 ml samples were used for each experiment. The samples were degassed to remove unbound sulfide and then fractionated on a Sephadex G-25 column (1.6×30 cm) equilibrated with 10 mM Tris.Cl (pH 8.6). Fractions (~1.5 ml) eluting from the column were analyzed for Zn, -SH and sulfide concentrations using atomic absorption spectrophotometry (Perkin-Elmer Model 3100), 2,2′dithiodipyridine titration (19) and methylene blue reduction assays (20), respectively. The determination of -SH groups in sulfide containing samples was carried out after sulfide was dissociated by acidification (with HCl to pH ~1.0) and removed by degassing. Additional experiments showed that the concentrations of reduced GSH determined thus were similar to those estimated by the cyclic assay (21). The samples lacking any added sulfide were fractionated on Sephadex G-10 equilibrated with 10 mM Tris. Cl (pH 8.6). Column fractions were diluted with 10 mM Tris.Cl (pH 8.6) to obtain ~10 μg Zn/ml for recording absorption spectra as mentioned above. The luminescence spectra of the diluted samples were recorded on a Perkin-Elmer LS 50B spectrofluorimeter controlled by FLDM software. All luminescence spectra were recorded following excitation of the samples at 270 nm. The absorption and luminescence spectra were converted into ASCII files using PECSS and FLDM software, respectively. The scanned samples were reanalyzed for Zn,-SH and sulfide concentrations using procedures mentioned above.

Reduction of methylviologen. GSH-ZnS samples from different sulfide titrations were titrated with NaOH to pH 11.0 prior to mixing with methylviologen (10). Zn and methylviologen concentrations were adjusted to 0.15 and 0.2 mM, respectively. The samples (2.0 ml) were transferred to septum-sealed cuvettes (Spectrocell Inc.), thoroughly degassed and saturated with N_2. These cuvettes were sealed inside the anaerobic chamber. The absorption spectra were recorded prior to irradiation that was performed by placing the cuvettes next to a short-wave (254 nm) UV lamp (UVP, Inc. Model UVGL-25) for predefined time intervals. The irradiated samples were scanned for spectral changes after each irradiation. Similar experiments were carried out using samples that were not degassed to remove oxygen.

Effects of pH on spectral properties of GSH-ZnS. Selected samples were diluted in potassium phosphate solutions at various pH values to obtain Zn concentrations of 5μg/ml. Potassium phosphate solutions in the pH range 3-13 were prepared by titrating 50 mM phosphoric acid with 1M KOH. The electronic absorption and luminescence spectra were recorded as described above.

RESULTS AND DISCUSSION

Sulfide-induced changes in absorption spectrum of Zn-GSH. Cd(II)-forms of both GSH and PCs incorporate inorganic sulfide to form complexes that exhibit characteristics of CdS nanocrystallites (9,10,14). These complexes are formed *in vivo* and can also be assembled *in vitro* (9,10,14,22). The incorporation of sulfide into

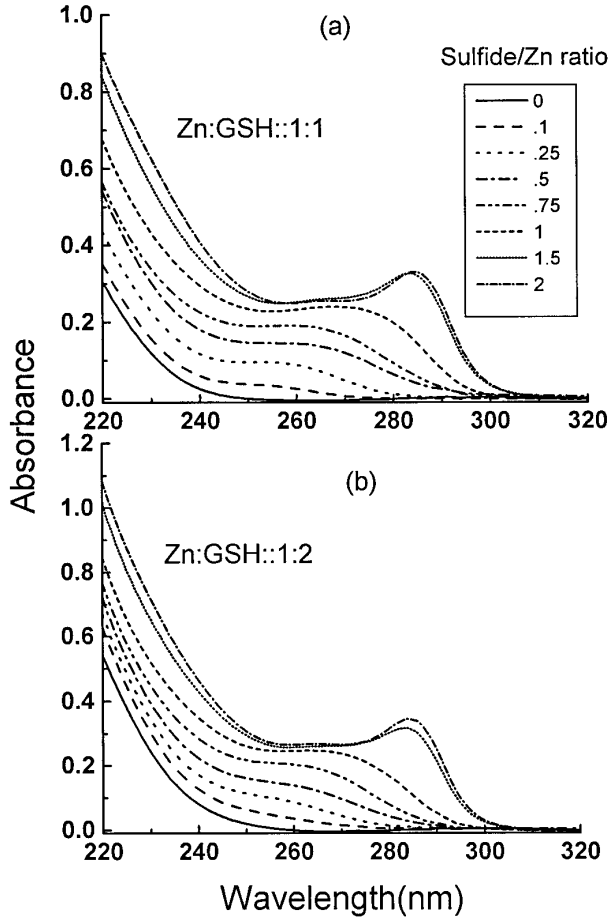

FIG. 1. Sulfide-induced spectral changes in Zn-GSH. The metal-glutathione complexes at Zn/GSH ratios of 1.0 (a) and 0.5 (b) were prepared as detailed in the text. Sulfide titrations were performed in increasing equivalents as indicated by the key in (a). The final Zn concentration in each of these samples was 100 μM.

Cd-GSH and Cd-PCs leads to the development of absorption shoulders in 280-350 nm range; higher sulfide containing samples have the most red-shifted shoulders (9,10,14,22). These spectral features also led to the identification of these complexes as nanocrystallites (14). Thus, analysis of sulfide-induced changes in the absorption spectra was the first step in determining whether Zn-GSH incorporated sulfide. As shown in Fig. 1 (a,b), the titration of 0.1equivalent sulfide (with respect to Zn) into Zn-GSH complexes led to the appearance of a shoulder at ~260 nm. This absorption band red-shifted upon titration of increasing equivalents of sulfide. The samples titrated with 2 equivalents of sulfide showed a small peak around 262 nm and a more pronounced peak around 285 nm. The sample containing equimolar amounts of Zn and GSH showed a slightly higher red-shifting. Later determinations (see below) showed that the samples titrated with 2 equivalents of sulfide incorporated only a maximum of one equivalent, the remainder was volatilized during de-

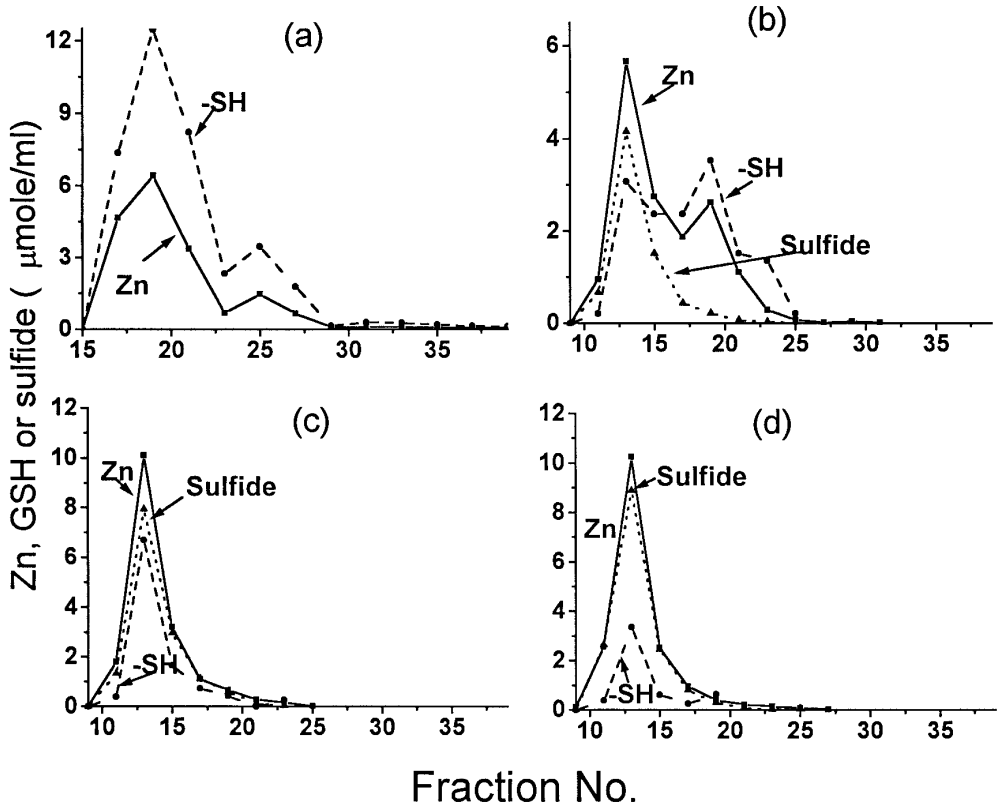

FIG. 2. Gel-filtration fractionation of Zn-GSH titrated with 0(a), 0.5 (b), 1.0(c) and 2.0(d) sulfide equivalents. Zn, free -SH and sulfide concentrations in alternate samples were determined and shown in the chromatograms. See text for details.

gassing. The absorption spectra shown in Fig. 1 (a,b) are similar to those reported for ZnS nanocrystallites (23), except the variations in GSH-ZnS samples that appeared to depend on sulfide content.

Size-fractionation of GSH–ZnS complexes. It has been shown that an increase in the size of nanocrystallites leads to red-shifting of the absorption shoulders (24). The fractionation of *in vivo* formed CdS nanocrystallites on gel-filtration columns also showed that higher molecular weight fractions contained most sulfide and exhibited maximally red-shifted absorption shoulders (9,10,14,22). Thus, gel-filtration fractionation of GSH-ZnS complexes was carried out to determine if these complexes also exhibited size- and sulfide-dependent changes in spectra. In addition, these experiments allowed determination of precise stoichiometries of Zn,GSH and sulfide in size-fractionated samples. Experiments were carried out using Zn/GSH ratios of 0.25, 0.5 and 1.0. However, only the data from $Zn_1(GSH)_2$ complex are presented here as results were generally similar with different stoichiometries. Zn(II) forms a variety of complexes with GSH and the nature of such complexes varies with pH (17). Gel-filtration of Zn-GSH (Zn:GSH::1:2) complex showed two peaks of Zn and both peaks contained titratable -SH groups (Fig. 2a). The peak fraction in the major peak showed -SH/Zn ratio of 1.9, whereas the peak fraction in the minor peak showed -SH/Zn ratio of 2.4. Overall, the early eluting fractions had a lower -SH/Zn than the late eluting fractions. These results are similar to the observations made using titration or NMR techniques that suggested formation of a variety of Zn-GSH complexes (17).

The titration of 0.5 equivalent sulfide showed two peaks containing Zn (Fig. 2b). The higher molecular weight peak contained most of the sulfide, whereas only minimal amounts of sulfide were present in the second peak. The sulfide/Zn ratio was ~0.7 in the higher molecular weight fraction. The sulfide containing fractions showed Zn/GSH ratios greater than 2 indicating a substantial increase in the metal-binding capacity of this peptide. The titration of 1.0 equivalent of sulfide (with respect to Zn) showed that all the metal and sulfide was now present in one peak (Fig. 2c). The sulfide/Zn ratio increased to about 0.8 in the peak fraction, with the earlier fractions containing somewhat higher ratios. $Zn_1(GSH)_2$ sample titrated with 2.0 equivalents of sulfide exhibited Zn/GSH ratios varying from 3 to 7 and sulfide/Zn ratios varying from 0.86 (in peak fraction) to 1.0 in the earliest eluting fractions (Fig. 2d). Only the Zn containing fractions were assayed for -SH and, therefore, free GSH liberated upon titration of increasing quantities of sulfide is not shown in these chromatograms.

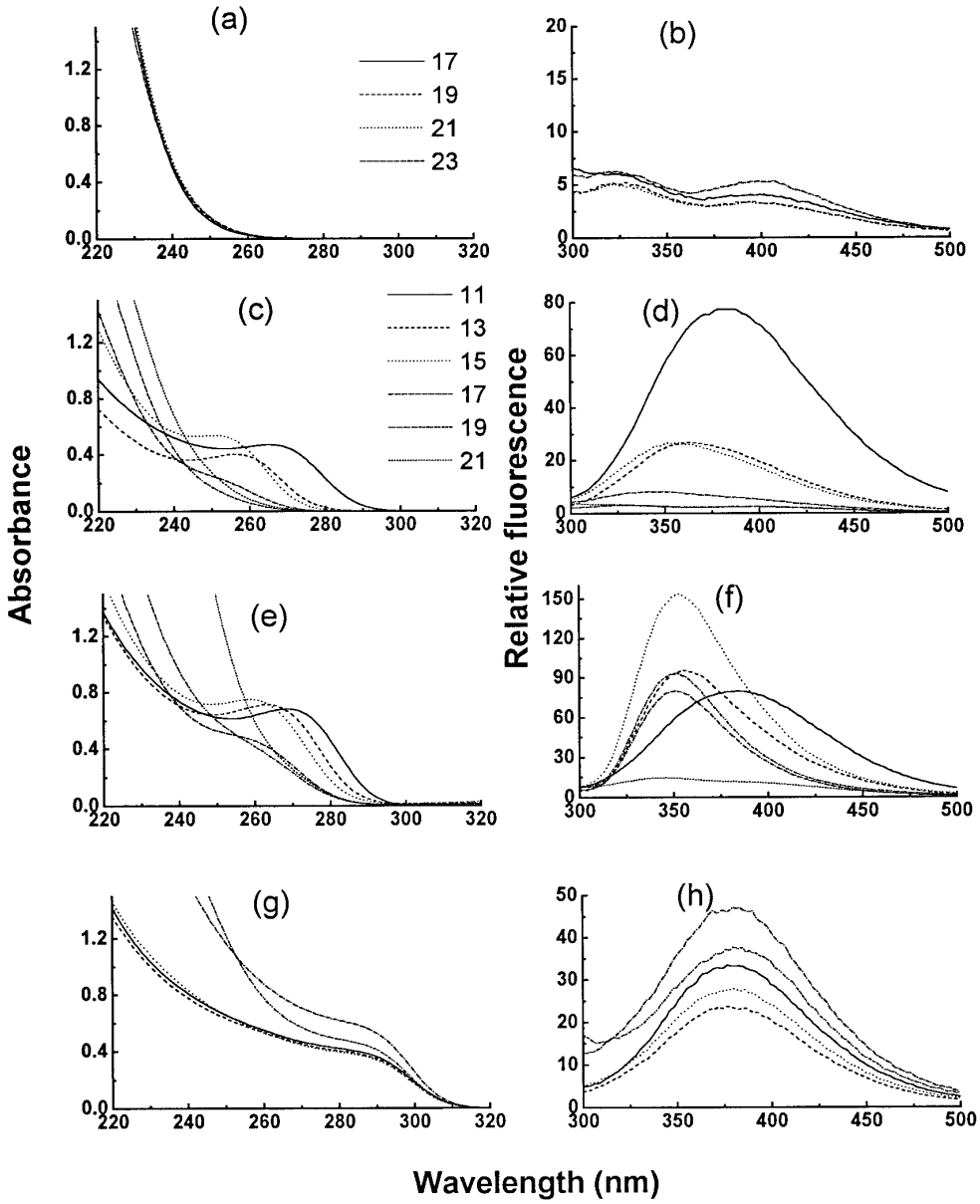

FIG. 3. UV/VIS (a,c,e,g) and luminescence (b,d,f,h) spectra of Zn containing fractions obtained from chromatograms shown in Fig. 2. Spectra for fractions from 0 S titration (a,b), 0.5 S titration (c,d), 1.0 S titration (e,f) and 2.0 S titration (g,h) are shown. Each of the samples contained 10 μg Zn/ml. Same key is used for spectra obtained for individual fractions from each of the column fractions, except for 0 S titration, and is shown in (c). The key for 0 S titration is shown in (a).

Spectral properties of GSH–ZnS fractions varying in sulfide content. That a variety of GSH-ZnS complexes were formed even with a given sulfide titration was indicated by variations in the stoichiometries of the three components in different column fractions (cf. Fig. 2). Absorption and luminescence spectroscopy confirmed that individual fractions indeed contained different species (Fig. 3a-h). Zn-GSH fractions eluting from Sephadex G-10 in the absence of added sulfide showed identical UV/VIS spectra and very similar luminescence spectra (Fig. 3a,b). The small luminescence peak at 325 nm might be due to a carry-over of the Raman scattering. The significance of a weak band at 400 nm is unclear at present. Analyses of fractions obtained from $Zn_1(GSH)_2$ sample titrated with 0.5 equivalent sulfide showed that the earliest eluting fraction (sulfide/Zn=0.7) had an absorption at ~270 nm. This shoulder blue-shifted with the decreasing size of complexes (later eluting fractions) such that the last fraction (number 17) showed the sulfide-induced shoulder at ~252 nm (Fig. 3c). Fraction number 17 exhibited a sulfide/Zn ratio of only 0.22. The emission characteris-

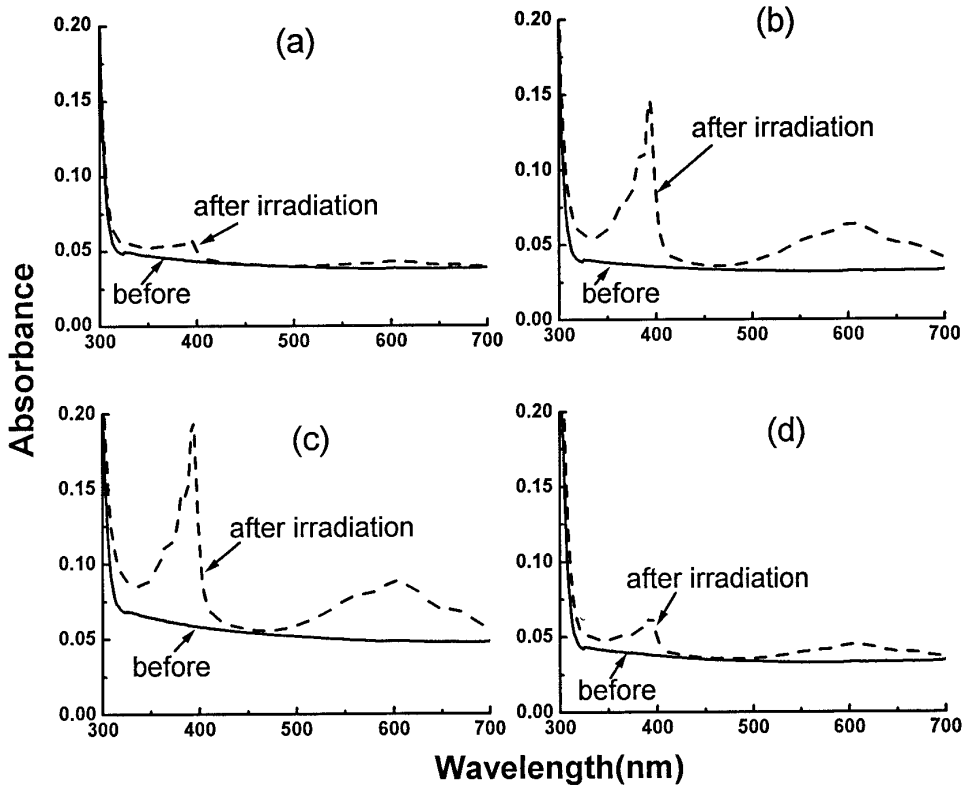

FIG. 4. Methylviologen reduction by Zn-GSH (a) or GSH-ZnS (b-d). Spectra of samples obtained before irradiation (solid line) and after irradiation for 20 min are shown for the fractions from 0 S (a), 0.5 S (b), 1.0 S (c) and 2.0 S (d) titration. The final Zn concentration in each experiment was 10 μg/ml. See the text for more details.

tics of these fractions (Fig. 3d) showed highest luminescence for fraction number 13; the emission band was centered around 375 nm. There was a continuous blue-shift in the emission of the later eluting fractions with lower molecular weights. Similar spectral features were seen in the fractions from sample titrated with 1.0 equivalent sulfide (Fig. 3e,f). These samples showed further red-shifting of the absorption shoulder to a maximum of 272 nm in the earliest eluting fraction. The sulfide/Zn ratios varied from 0.8 to 0.22 in fractions showing a clear sulfide-induced transition. The emission spectra of these complexes (Fig. 3f) followed the absorption spectra in that the emission maxima were shifted to the blue with decreasing sulfide/Zn ratios. $Zn_1(GSH)_2$ sample titrated with 2.0 equivalents of sulfide showed that a majority of the fractions had a similar absorption spectrum with a shoulder at ~290 nm and only a slight blue-shift occurred in the lower molecular weight complexes eluting later (Fig. 3g,h). Nearly all of these fractions had similar luminescence profiles, although the emission yields were different. The sulfide/Zn ratios in these fractions varied from 0.7 to 1.0.

The gel-filtration data and the spectroscopic data on individual fractions established that a range of GSH-ZnS complexes were formed and the sulfide/Zn ratios determined the characteristics of the optical spectra. The highest sulfide/Zn ratios were close to 1.0 and these complexes exhibited UV/VIS transitions in the 290 nm range, the transitions blue-shifted with the decreasing quantities of sulfide incorporated. These observations are very similar to those recorded for GSH-CdS (10) and PC-CdS crystallites (9), except that the absorption and the emission bands are significantly blue-shifted in GSH-ZnS complexes in comparison with GSH-CdS crystallites. ZnS nanocrystallites prepared by mixing zinc nitrate and sodium sulfide in the absence of any capping material showed absorption shoulder around 264nm and had a broad emission band at 435 nm (23). The absorption bands of GSH-ZnS complexes are similar to the uncapped ZnS nanocrystallites, but the emission bands are significantly blue-shifted. As the emission of nanocrystallites is due to recombination of photogenerated electrons and holes (23), it seems reasonable to assume that the functional groups of the capping GSH might have introduced modifications in the emission spectra observed in our studies.

GSH–ZnS crystallites reduce methylviologen. The semiconductor nature of GSH-ZnS complexes was further confirmed by reduction of methylviologen by these complexes (9,10). Irradiation of a mixture of GSH-ZnS complexes and methylviologen with UV light at 254

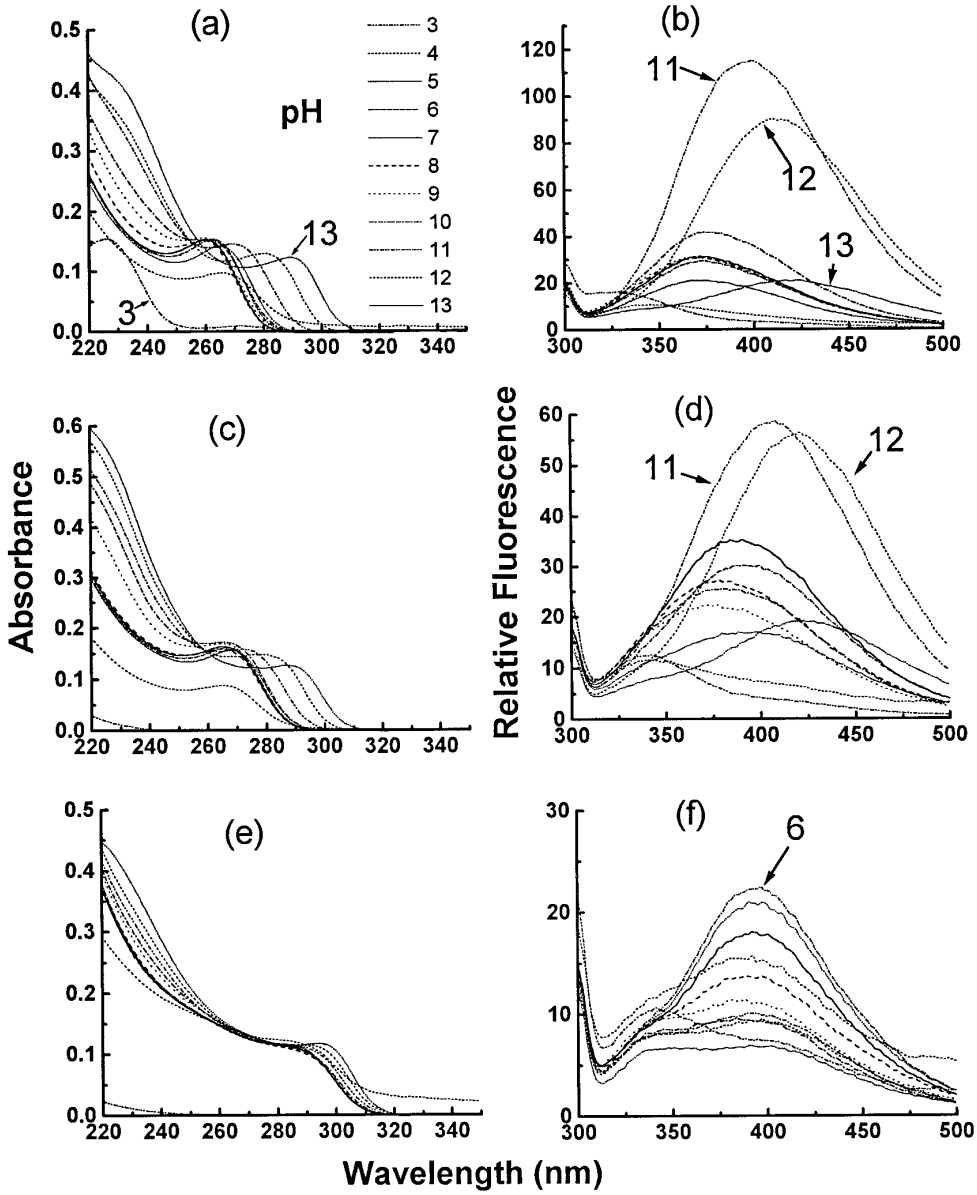

FIG. 5. Effect of pH on absorption (a,c,e) and luminescence (b,d,f) spectra of GSH-ZnS samples obtained from 0.5 S (a,b), 1.0 S (c,d) and 2.0 S (e,f) titration. Peak fraction (number 13) was used for each experiment and Zn concentration in each sample was adjusted to 5 μg/ml.

nm did not lead to any noticeable reduction of the dye under aerobic conditions (data not shown). However, the irradiation of anaerobic samples from different sulfide titrations showed clear evidence of methylviologen reduction as indicated by the appearance of the characteristic spectrum of reduced methylviologen (Fig. 4a-d). It is intriguing that $Zn_1(GSH)_2$ by itself caused slight but observable reduction of the electron acceptor (Fig. 4a). Several different samples of $Zn_1(GSH)_2$ with or without gel-filtration were able to show a perceptible reduction of the dye. However, $Cd_1(GSH)_2$ did not show any reduction of methylviologen (data not shown, 10). Samples containing ~0.7 to ~0.8 sulfide/Zn were more effective (Fig. 4b,c) than those containing ~0.9 sulfide/Zn (Fig. 4d) in the reduction of methylviologen.

pH-dependence of spectral characteristics of GSH–ZnS crystallites. The optoelectronic properties of metal-sulfide nanocrystallites are size-dependent (23,24). One of the factors that influences the size and thus the optical properties is the pH (9,10,14,23,24). Acidification leads to aggregation of nanoparticles with the resultant red-shifting of the absorption shoulder and of the luminescence bands. Our previous studies on the accumulation of CdS particles within the *Candida glabrata* cells showed that highly luminous microscopic particles accumulated in vacuoles which are acidic rela-

tive to the cytosolic compartment (22). Uncapped ZnS nanocrystallites showed maximal luminescence at pH 6.0 (23). However, GSH-capped ZnS nanocrystallites showed GSH-dependent changes in the optical spectra as the pH was varied (Fig. 5a-f). Peak gel-filtration fractions (number 13 from each of the runs shown in Fig. 2) from 0.5 (sulfide/Zn ratio =0.73),1.0 (sulfide/Zn ratio 0.79) and 2.0 sulfide (sulfide/Zn ratio=0.87) titrations were adjusted to pH values from 3-13 and scanned for absorption and luminescence spectra. At the extreme acidic pH, complexes dissociated and the released sulfide could be smelt. The sample from 0.5 sulfide titration showed ~268nm band at pH 5 and 6. This band blue-shifted to 262 nm at pH 7-9. Further increase in alkalinity led to a dramatic red-shifting with shoulder appearing at 290 nm at pH 13 (Fig. 5a). The luminescence of the same sample showed a 370 nm emission band with less intensity at pH 5 than at pH 6-9. A red-shifting occurred as the pH was changed to 10; maximal luminescence occurred at pH 11 and had a broad band at ~390 nm. Luminescence declined at higher alkaline pHs with a concomitant change in the λ_{max} to ~405 nm. Qualitatively similar changes were recorded for pH dependence of the sample with 1.0 sulfide titration (Fig. 5c,d). However, this sample showed increased red-shifting of the absorption and emission bands as compared with 0.5 sulfide sample. In sharp contrast to the above results, the sample from 2.0 molar equivalent sulfide (sulfide/Zn ratios = 0.86 to 1.0) showed only minor variations in the absorption spectra between pH 6-10. Only a slight red-shifting occurred at higher pHs. More strikingly, the luminescence yield was highest at pH 6 and decreased on either side of this pH. Only very minor qualitative changes were seen in the luminescence spectra at different pHs for high sulfide samples.

The spectral changes described above for higher GSH-containing samples (1.0 Zn, 0.8 sulfide, 0.5 GSH) differ considerable from the data on uncapped ZnS nanocrystallites (23). It is important to note that the sample with least glutathione and highest sulfide (~1.0 Zn, ~0.86 sulfide and 0.3 GSH) behaved like uncapped ZnS nanocrystallites, although emission λ_{max} was still slightly to the blue of the reported 435 nm band for uncapped materials. As mentioned above, the red-shifting in nanocrystallites is generally due to a process termed Ostwald ripening that causes aggregation of the smaller particles. This process is accelerated by acidic pH and increased temperatures (9,10,23,24). However, the red-shifting seen in GSH-capped ZnS crystallites with increasing pH is probably due to ionizing changes occurring in the capping GSH molecule. Electron-microscopic studies are needed to resolve this issue.

In conclusion, we have shown that Zn-GSH incorporates inorganic sulfide to form a variety of complexes. These complexes are separable on size-fractionation columns. An increase in sulfide/Zn ratios from 0 to about 1.0 increases Zn/GSH ratio from about 0.5 to 7.0 indicating a 14-fold increase in Zn-binding capacity of GSH. The spectral characteristics (and thus the opto-electronic properties) of the bionanocrystallites comprising GSH-ZnS can be varied easily by controlling the amounts of sulfide titrated into preformed Zn-GSH complex. These complexes can find a wide variety of applications including possible use in degradation of toxic organic contaminants. Recent studies have suggested the use of CdS particles for the free-radical mediated degradation of organic contaminants (15,16) and in the analysis of bends and kinks in DNA (25). However, Cd is highly toxic and unsuitable for waste-treatment purposes. GSH-based bionanocrystallites described here would appear to be a better choice for waste-treatment and possibly for analysis of alterations in DNA structure.

ACKNOWLEDGMENTS

This work was supported in part by funds awarded to R.K.M. by the Air Force Office of Scientific Research (F 49620-94-1-0047), UC Toxic Substances Teaching & Research Program and the University of California, Riverside, Academic Senate. W.B. was supported in part by the Environmental Toxicology Graduate Program, University of California, Riverside. We thank Drs Harry Tom, Umar Mohideen, Victor Klimov and Radha Ranganathan for stimulating discussions. We thank Christina Shin, Tom Hunter and other member of our laboratory for constructive criticism and assistance in some experiments.

REFERENCES

1. Commandeur, J. N. M., Stijntjes, G. J., and Vermeulen, N. P. E. (1995) *Pharmacological Reviews* **47,** 271–330.
2. Winkler, B. S., Orselli, S. M., and Rex, T. S. (1994) *Free Radical Biology & Medicine* **17,** 333–349.
3. Singhal, R. K., Anderson, M. E., and Meister, A. (1987) *FASEB J.* **1,** 220–223.
4. Mehra, R. K., Kodati, V. R., and Abdullah, R. (1995) *Biochem. Biophys. Res. Comm.* **215,** 730–736.
5. Mehra, R. K., and Mulchandani, P. (1995) *Biochem. J.* **307,** 697–705.
6. Mehra, R. K., Miclat, J., Kodati, V. R., Abdullah, R., Hunter, T. C., and Mulchandani, P. (1996) *Biochem. J.* **314,** 73–82.
7. Ferreira, A. M., Ciriolo, M. R., Marcocci, L., and Rotilio, G. (1993) *Biochem. J.* **292,** 673–676.
8. Li, Z-S., Lu, Y. P., Zhen, R. G., Szczypka, M., Thiele, D. J., and Rea, P. A. (1997) *Proc. Natl. Acad. Sci. (USA)* **94,** 42–47.
9. Dameron, C. T., and Winge, D. R. (1990) *Inorg. Chem.* **29,** 1343–1348.
10. Dameron, C. T., Smith, B. R., and Winge, D. R. (1989) *J. Biol. Chem.* **264,** 17355–17360.
11. Speiser, D. M., Ortiz, D. F., Kreppel, L., Scheel, G., McDonald, G., and Ow, D. W. (1992) *Mol. Cell Biol.* **12,** 5301–5310.
12. Ortiz, D. F., Kreppel, L., Speiser, D. M., Scheel, G., McDonald, G., and Ow, D. W. (1992) *EMBO J.* **11,** 3491–3499.
13. Mutoh, N., and Hayashi, Y. (1988) *Biochem. Biophys. Res. Comm.* **151,** 32–39.
14. Dameron, C. T., Reese, R. N., Mehra, R. K., Kortan, A. R., Carroll, P. J., Steigerwald, M. L., Brus, L. E., and Winge, D. R. (1989) *Nature* **338,** 596–598.

15. Tseng, J. M., and Huang, C. P. (1991) *Water Sci. Tech.* **23,** 377–387.
16. Tang, W. Z., and Huang, C. P. (1995) *Water Res.* **29,** 745–756.
17. Rabenstein, D. L., Guevremont, R., and Evans, C. A. (1979) *in* Metal Ions in Biological Systems (Segel, H., Ed.), Vol. 9, pp. 103–141, Dekker, New York.
18. Barbas, J., Santhanagopalan, V., Blaszczynski, M., Ellis, W. R., Jr., and Winge, D. R. (1992) *J. Inorg. Biochem.* **48,** 95–105.
19. Grassseti, D. R., and Murray, J. F. (1967) *Arch. Biochem. Biophys.* **119,** 41–49.
20. King, T., and Morris, O. (1957) *Methods Enzymol.* **10,** 636–641.
21. Anderson, M. E. (1985) *Methods Enzymol.* **113,** 548–555.
22. Mehra, R. K., Mulchandani, P., and Hunter, T. C. (1994) *Biochem. Biophys. Res. Comm.* **200,** 1193–1200.
23. Sooklal, K., Cullum, B. S., Angel, S. M., and Murphy, C. J. (1996) *J. Phys. Chem.* **100,** 4551–4555.
24. Rossetti, R., Ellison, J. L., Gibson, J. M, and Brus, L. E. (1984) *J. Chem. Phys.* **80,** 4464–4469.
25. Mahtab, R., Rogers, J. P., and Murphy, C. J. (1995) *J. Am. Chem. Soc.* **117,** 9099–9100.